

This item is the archived peer-reviewed author-version of:

A Pareto aggregation approach for environmental-economic multi-objective optimization applied on a second-generation bioethanol production model

Reference:

Vasilakou Konstantina, Billen Pieter, Van Passel Steven, Nimmegeers Philippe.- A Pareto aggregation approach for environmental-economic multi-objective optimization applied on a second-generation bioethanol production model
Energy conversion and management - ISSN 1879-2227 - 303(2024), 118184
Full text (Publisher's DOI): <https://doi.org/10.1016/J.ENCONMAN.2024.118184>
To cite this reference: <https://hdl.handle.net/10067/2030460151162165141>

1 A Pareto aggregation approach for environmental-economic multi-objective optimization
2 applied on a second-generation bioethanol production model

3 Konstantina Vasilakou^{a,b,c,*}, Pieter Billen^b, Steven Van Passel^{a,c,d}, Philippe Nimmegeers^{a,b,c}

4 ^aEnvironmental Economics (EnvEcon), Department of Engineering Management, Faculty of
5 Business and Economics, University of Antwerp, Prinsstraat 13, 2000 Antwerp, Belgium.

6 ^bIntelligence in Processes, Advanced Catalysts and Solvents (iPRACS), Faculty of Applied
7 Engineering, University of Antwerp, Groenenborgerlaan 171, 2020 Antwerp, Belgium.

8 ^cFlanders Make@UAntwerp, 2000 Antwerp, Belgium

9 ^dNanolab Centre of Excellence, Prinsstraat 13, 2000 Antwerp, Belgium.

10 *E-mail addresses: konstantina.vasilakou@uantwerpen.be (K. Vasilakou),*
11 *pieter.billen@uantwerpen.be (P. Billen), steven.vanpassel@uantwerpen.be (S. Van Passel),*
12 *philippe.nimmegeers@uantwerpen.be (P. Nimmegeers).*

13 **ABSTRACT**

14 Multi-objective optimization is an important decision-making tool for energy processes, as
15 multiple targets need to be achieved. These objectives are usually conflicting since a single
16 solution cannot be optimal for all objectives, resulting in a set of Pareto-optimal solutions.
17 Multiple indicators might be available to describe a sustainability objective, such as the
18 environmental impact which is commonly evaluated by performing a life cycle assessment. In
19 this study, Pareto aggregation is proposed as a method which employs a novel multi-objective

*Corresponding Author at: Environmental Economics (EnvEcon), Department of Engineering Management, Faculty of Business and Economics, University of Antwerp, Prinsstraat 13, 2000 Antwerp, Belgium. E-mail address: konstantina.vasilakou@uantwerpen.be

20 optimization-based approach as an alternative to the classically used aggregation in life cycle
21 assessment. This method identifies conflicting environmental indicators and performs an
22 aggregation among those that require a trade-off. An environmental-economic optimization of
23 a second-generation bioethanol plant is used to illustrate and evaluate the proposed method.
24 Process parameters from a biochemical conversion pathway flowsheet simulation model are
25 chosen as optimization variables. To reduce the computational time, surrogate models, based
26 on artificial neural networks, are used. Out of the eighteen ReCiPe Midpoint environmental
27 indicators, five were identified as conflicting, resulting in an aggregated environmental
28 objective, which was then traded off with the economic objective function, chosen as the
29 levelized cost of ethanol. Comparison with the widely used single-score EcoIndicator99
30 showed that the Pareto aggregation method can reduce most of the environmental indicators by
31 up to 6.5%. This research provides an insight on non-redundant objective functions, aiming at
32 reducing the dimensionality of multi-objective optimization problems, while taking into
33 consideration decision-makers' preferences.

34 **KEYWORDS**

35 Multi-objective optimization, sustainability optimization, life cycle assessment, bioprocess
36 modelling, biorefinery

37 **NOMENCLATURE**

38 *Abbreviations*

39 ANN: Artificial neural network

40 BP: Best point

41 CAPEX : Capital expenditure

- 42 LCA: Life cycle assessment
- 43 MOO: Multi-objective optimization
- 44 MSE: Mean squared error
- 45 OPEX: Operational expenditure
- 46 *Symbols*
- 47 a : annuity factor
- 48 C_{FCI} : fixed capital investment (EUR)
- 49 $C_{operlab}$: operating labor cost (EUR/h)
- 50 C_{opfix} : fixed operating cost (EUR/y)
- 51 C_{opvar} : variable operating cost (EUR/y)
- 52 \tilde{J}_i : predicted value of J_i
- 53 J_i^{BP} : objective value of J_i on the Best point
- 54 $J_{agg,env}$: aggregated environmental objective
- 55 J_{conf} : set of conflicting objectives J_i
- 56 J_{env} : set of environmental objectives J_i
- 57 J_i : objective function i
- 58 $J_i^{BP,EI99}$: objective value of J_i on the Best point of the EcoIndicator99-economic Pareto front

- 59 $J_i^{BP,agg}$: objective value of J_i on the Best point of the aggregated environmental-economic
60 Pareto front
- 61 J_{obj} : set of objective functions
- 62 k : number of objectives for each combination
- 63 LCE : levelized cost of ethanol (EUR/L)
- 64 N : number of Pareto fronts
- 65 n : number of samples
- 66 n_j : number of objective functions J
- 67 n_{JC} : number of conflicting objectives J_i
- 68 n_{Jenv} : number of environmental objectives
- 69 P_{EtOH} : annual ethanol production (L/y)
- 70 PF_{JC} : number of conflicting Pareto fronts
- 71 W_i : weights of each conflicting objective $J_i \in J_{conf}$
- 72 x : vector of optimization variables
- 73 x_{max} : vector of the maximum values of the optimization variables
- 74 x_{min} : vector of the minimum values of the optimization variables
- 75 y_i : variable of min-max scaling
- 76 y'_i : normalized value of y_i variable

77 U : Utopia point of two objective functions J_i and $J_{j \neq i}$

78 1. INTRODUCTION

79 During the design and operation of energy systems, decisions have to be taken
80 considering multiple objectives, namely: maximizing economic performance (e.g., Net Present
81 Value (NPV), profit), while minimizing environmental impact (e.g. global warming potential,
82 carbon footprint, ecosystem quality savings) [1]. These objectives can be conflicting, as
83 improving one can result in worsening the other. In such a situation, there is not one optimal
84 solution, but rather several mathematically equivalent trade-off solutions exist (i.e., Pareto
85 optimal solutions) [2]. Multi-objective optimization (MOO) methods generate such a set of
86 Pareto optimal solutions, called the Pareto front [3], and have been widely used in energy
87 applications [4]. These mathematically equivalent trade-off solutions can then assist in the
88 decision-making process. The systematic generation and efficient presentation of these optimal
89 alternatives to decision-makers plays a key role in computer-aided decision making. Decisions
90 need to be made in an efficient and well-informed manner while the decision-makers'
91 preferences also need to be taken into account [1].

92 In environmental assessments, such as the widely used life cycle assessment (LCA),
93 many different indicators are exploited to quantify and evaluate environmental impacts [5].
94 Usually only CO₂ emissions are taken into consideration in multi-objective optimization
95 problems on energy systems [6,7], neglecting the rest of the indicators. On the other hand,
96 multiple environmental indicators can be normalized and weighted, resulting in a single score
97 indicator. The use of a single aggregated indicator facilitates the communication and
98 interpretation of the comparative results from LCA practitioners to decision-makers [8]. For
99 example, endpoint impact categories (i.e., damages to human health, ecosystem quality and

100 resources) are used to have a comprehensive view on environmental impacts [9]. Then, these
101 impact categories are often aggregated into a single Eco-Indicator [10] (e.g., Eco-indicator 99
102 [9]).

103 However, the weighted sum procedure has received lot of criticism over the years, due
104 to the danger of incorrectly interpreting the weighted results, as weighting factors are subjective
105 and might not represent decision-makers' preferences [8,11]. As a result, multiple efforts have
106 been made to improve the aggregation approach in environmental assessments. Afrinaldi et al.
107 [8] have proposed a novel method for normalization and aggregation in LCA based on fuzzy
108 logic, which was applied in automotive engines. Similarly, Agarski et al. [12] have used fuzzy
109 logic for impact category weighting in an LCA study on waste treatment processes. The
110 analytical hierarchy process (AHP) has also been applied to estimate weighting factors for an
111 electricity generation case study [11]. Moreover, Sohn et al. [13] have developed a novel
112 weighting method, called Argumentation Corrected Context Weighting-LCA (ArgCW-LCA),
113 which uses multi-criteria decision analysis to aggregate midpoint impacts to a single indicator.

114 Despite these efforts, the use of aggregated impact indicators as the final environmental
115 objective function in optimization problems, can lead to suboptimality and a loss of information
116 for decision makers [14,15]. Indeed, the attained solution of the problem is influenced by the
117 weighted sum procedure as the conflicting behavior of different impact categories is not
118 considered, leading to suboptimal solutions. A recent study by Zacharopoulos et al. [16] focused
119 on optimizing battery electric vehicles (BEV) charging profiles by minimizing their
120 environmental impact, while also including the identification of conflicting and non-conflicting
121 environmental midpoint impact indicators. The conflicting indicators were determined by first
122 optimizing each impact indicator separately, then calculating the rest of the indicators for these
123 optimized charging profiles and finally measuring the deviation between the objectives. Despite

124 identifying conflicting environmental objectives, the aggregation of these conflicting indicators
125 into a single final environmental objective was not included in the study.

126 To address this knowledge gap, a novel method named *Pareto aggregation* is proposed
127 in this study which firstly solves systematically a multi-objective optimization problem related
128 to environmental sustainability using different indicators and identifying which indicators are
129 truly conflicting and between which ones a tradeoff needs to be made. In contrast to the current
130 state-of-the-art, by identifying the difference between conflicting and non-conflicting
131 objectives, the objective space is reduced by only retaining the conflicting ones, as the non-
132 conflicting ones will lead to the same optimal solution (and hence a waste of computational
133 power and time). Based on decision-maker preferences and/or the level of conflict between the
134 objectives, an aggregation is performed, resulting in one aggregated environmental objective,
135 which is then traded off against an economic objective function when solving a second bi-
136 objective environmental-economic optimization problem. This method is especially designed
137 to tackle in a systematic way multi-objective optimization formulations which are normally
138 solved via aggregation, although it is generally applicable to all types of MOO problems. Thus,
139 it can serve as a useful tool in decision-making processes, commonly encountered during the
140 design and operation of energy systems, when the technical, exergetic, economic,
141 environmental and/or social performances are often evaluated.

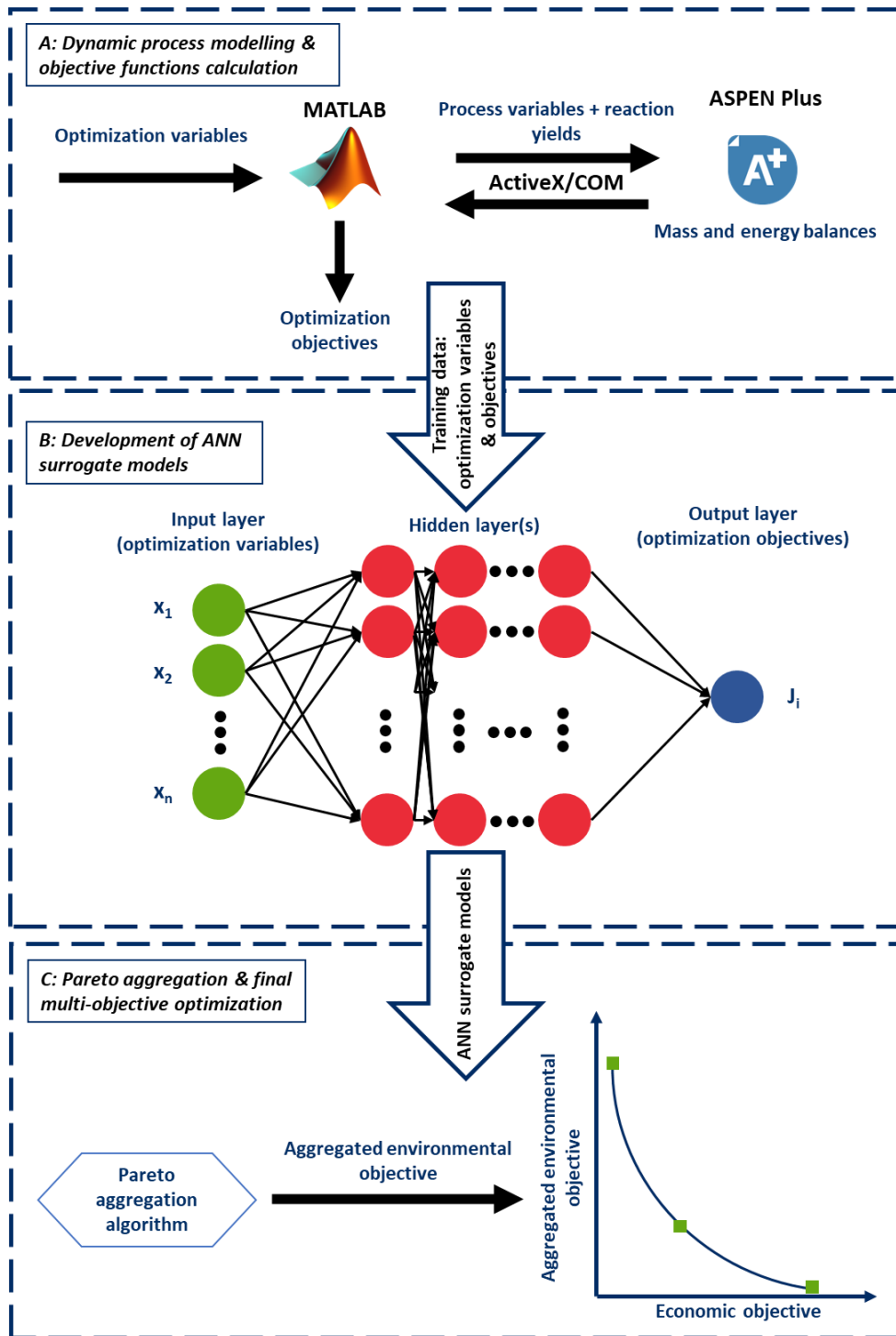
142 To illustrate this methodology, second-generation bioethanol production is chosen as a
143 realistic and complex energy conversion case study. Biomass has emerged as a renewable
144 energy resource with a high potential in the worldwide efforts for a greener energy transition
145 [17]. Out of its various applications, the production of biofuels can assist in achieving future
146 climate targets and meeting energy demand [18]. In particular, lignocellulosic biomass is an
147 abundant carbon source, rich in energy components that can be converted to biofuels,

148 commonly known as second-generation biofuels [19]. Due to its recalcitrant structure, the
149 bioconversion of lignocellulose requires multiple complex processes [20]. The optimization of
150 such energy conversion systems has been an area of interest for the past years, with numerous
151 studies focusing on the optimal process design of biofuels production with respect to economic
152 and environmental criteria [21]. Dynamic process models are developed for the upstream
153 processes, those being dilute acid pretreatment, enzymatic hydrolysis and fermentation, by
154 using already developed kinetic models. Due to their complexity and long computational time,
155 surrogate models are developed and used instead [22], calculating the final optimization
156 objectives. In addition to this case study, the Pareto aggregation method can easily be applied
157 to different types of MOOs and systems. Its applicability is explained further in subsection
158 3.4.1, along with specific directions and requirements.

159 **2. MATERIAL AND METHODS**

160 The proposed methodology consists of three steps, indicated by A, B and C in Figure 1.
161 First, rigorous process models are developed to calculate mass and energy balances which are
162 the basis for the environmental and economic objective functions (Figure 1 (A)). For the
163 lignocellulosic bioethanol production these models are developed in ASPEN Plus, by using
164 kinetic models available in literature. Through an interface connection between ASPEN Plus
165 and MATLAB, the final economic and environmental objectives are calculated. Due to the
166 computationally expensive interface between ASPEN Plus and MATLAB and time required to
167 solve multi-objective optimization problems, artificial neural networks (ANN) are developed
168 as surrogate models for each objective function (Figure 1 (B)). As such the computational cost
169 to evaluate objective functions is reduced and the optimizations can be conducted efficiently.
170 The development of surrogate models is also highly relevant when more complicated models
171 are used that require more computational time. Finally, the Pareto aggregation method is

172 applied in order to calculate the final aggregated environmental objective, which is then traded
173 off against the economic objective (Figure 1 (C)) through a multi-objective optimization. A
174 detailed description of each methodology step is given in the next subsections.



175

176 Figure 1. Schematic overview of the methodology steps applied: (A) Dynamic process
 177 modelling and calculation of objective functions, (B) Development of ANN surrogate models,
 178 (C) Pareto aggregation and multi-objective optimization.

179 2.1 Rigorous process model development & simulations

180 Bioethanol production from corn stover is simulated in ASPEN Plus[®] v.12.1 [23], based
181 on the model of the National Renewable Energy Laboratory (NREL) [24]. Three main upstream
182 processes are included: dilute acid pretreatment, enzymatic hydrolysis and co-fermentation.
183 Dilute acid pretreatment was modelled according to Shi et al. [25] for hemicellulose
184 degradation, while the solubilization of lignin according to Lavarack et al. [26]. Following the
185 model of Humbird & Aden [27], a two-stage pretreatment process was assumed with 70%
186 conversion of oligomers to monomers. The kinetic model of Kadam et al. [28] was used for the
187 enzymatic hydrolysis (saccharification), assuming three main reactions with competitive
188 inhibition. Finally, co-fermentation by recombinant *Zymomonas mobilis* was assumed for the
189 final process, applying the kinetic model of Leksawasdi et al. [29].

190 Thus, all reaction yields are estimated based on the kinetic models used for each process
191 (see Supporting Material). The developed Ordinary Differential Equation (ODE) and
192 Differential Algebraic Equation (DAE) systems are solved in MATLAB R2022b with the built-
193 in ode15s function, transferring the calculated reaction yields to ASPEN, through an ActiveX
194 interface connection.

195 2.2 Economic indicator calculation

196 The levelized production cost of ethanol (LCE, EUR/L) is chosen as the main economic
197 indicator, calculated using equation (1) [30]:

$$LCE = \frac{(CAPEX \cdot \alpha + OPEX)}{P_{EtOH}} \quad (1)$$

198 Where CAPEX is the capital expenditure (EUR), OPEX the operational expenditure (EUR/y),
199 α the annuity factor (y^{-1}) and P_{EtOH} the annual ethanol production (L/y). The annuity factor is

200 calculated assuming 20 years of project lifetime and 15% discount rate [30], for a production
201 plant starting its operation in 2022.

202 The CAPEX is calculated by summing the fixed capital investment C_{FCI} (EUR), the
203 working capital (5% of the C_{FCI}) and the land cost (2% of the C_{FCI}) [24]. The C_{FCI} consists of
204 the total direct and indirect costs. The OPEX is calculated as the sum of the variable operating
205 (C_{opvar}) and the fixed operating (C_{opfix}) costs. Details on the input values and calculations are
206 given in the Supporting Material.

207 2.3 Environmental indicators calculation

208 The environmental performance is evaluated through a life cycle assessment (LCA).
209 The system covers the cultivation and supply of biomass, the supply of raw materials and energy
210 as well as the production of the final product. A cradle-to-gate approach is chosen, as the case
211 study is limited to the upstream processes of lignocellulosic ethanol (EtOH) production. The
212 functional unit is taken as 1 L of ethanol production. For the biomass cultivation, an economic
213 allocation is applied (11.3% for corn stover).

214 The EcoInvent database [31] and data on Belgian corn agriculture are used to develop
215 the life cycle inventory (see Supporting Material). The input and output flows are taken from
216 the ASPEN model and are expressed per L EtOH (i.e. the functional unit). The life cycle impact
217 assessment is performed in SimaPro[®] v.9.4.02, using the ReCiPe 2016 v1.1 Midpoint method
218 [32] and calculating eighteen environmental impact indicators.

219 For the validation of the suggested methodology, the EcoIndicator99 is also calculated,
220 using the ReCiPe 2016 v1.1 Endpoint method and its normalization factors, while weights are
221 taken from the methodology report on the EcoIndicator 99 [9]. This single score was chosen as
222 it is well recognized and widely used in relevant studies.

223 2.4 Multi-objective optimization problem formulation

224 Multi-objective optimization problems of the following form are studied in this work:

$$\min_x \{J_1(x, p), \dots, J_{n_j}(x, p)\} \quad (2)$$

225 subject to

$$226 \quad c(x, p) \leq 0$$

$$227 \quad x_{min} \leq x \leq x_{max}$$

228 With $J_{obj} = \{J_1(x, p), \dots, J_{n_j}(x, p)\}$ the n_j objective functions, $c(x, p)$ the constraint functions,
229 x the vector with optimization variables, p the model parameter vector, x_{min} the vector
230 containing the minimum values of the optimization variables and x_{max} the vector with the
231 maximum values of the optimization variables.

232 The solution of such a multi-objective optimization problem is a Pareto front of tradeoff
233 solutions. The Non-dominated Sorting Genetic Algorithm II (NSGA-II), an elitist evolutionary
234 algorithm, is used in this work. Problems are solved in MATLAB R2022b using the *gamultiobj*
235 function, taking function tolerance at 10^{-4} and constraint tolerance at 10^{-12} . All calculations were
236 performed using the Intel® Xeon® Gold 6334 CPU @ 3.60GHz – 3.59GHz (4 processors) and
237 16.0 GB RAM.

238 2.5 Surrogate modelling

239 Surrogate models are used for the calculation of the objective functions, as the coupling
240 of ASPEN and MATLAB is computationally expensive. Artificial Neural Networks (ANN) are
241 developed in this study for each objective function [33]. Thus, a set of 20 models is created, as
242 shown in Table 1.

243 Table 1. Objective functions for the multi-objective optimization of second-generation
 244 bioethanol production. J_1 is the economic indicator, J_2 - J_{19} are the environmental indicators and
 245 J_{20} is the EcoIndicator used for comparison.

Optimization objectives	Objective functions	Units
LCE	J_1	EUR/L
Global warming	J_2	kg CO ₂ eq/L
Stratospheric ozone depletion	J_3	kg CFC11 eq/L
Ionizing radiation	J_4	kBq Co-60 eq/L
Ozone formation, Human health	J_5	kg NO _x eq/L
Fine particulate matter formation	J_6	kg PM2.5 eq/L
Ozone formation, Terrestrial ecosystems	J_7	kg NO _x eq/L
Terrestrial acidification	J_8	kg SO ₂ eq/L
Freshwater eutrophication	J_9	kg P eq/L
Marine eutrophication	J_{10}	kg N eq/L
Terrestrial ecotoxicity	J_{11}	kg 1,4-DCB/L
Freshwater ecotoxicity	J_{12}	kg 1,4-DCB/L
Marine ecotoxicity	J_{13}	kg 1,4-DCB/L
Human carcinogenic toxicity	J_{14}	kg 1,4-DCB/L
Human non-carcinogenic toxicity	J_{15}	kg 1,4-DCB/L
Land use	J_{16}	m ² a crop eq/L
Mineral resource scarcity	J_{17}	kg Cu eq/L
Fossil resource scarcity	J_{18}	kg oil eq/L
Water consumption	J_{19}	m ³ /L
EcoIndicator 99	J_{20}	Points/L

246

247 2.5.1 Sampling and generation of training data

248 The training data required for the surrogate models are obtained by sampling the design
 249 space with the Best Candidate algorithm [34]. The chosen algorithm performs well and satisfies
 250 major requirements for surrogate modelling applications [35].

251 Feed rate, acid loading, pretreatment temperature, pretreatment residence time,
 252 saccharification residence time and fermentation residence time are the optimization variables
 253 chosen. The six-variable design space (6D) is sampled at once for 5000 samples, according to
 254 the permitted lower and upper bounds of Table 2. These limits are selected based on the

255 constraints of the kinetic models used for the process modelling, while ensuring that the
 256 simulation model runs without errors (simulation status was checked after each run). The
 257 generated samples are then used to run the simulation model and calculate the economic and
 258 environmental indicators. Since both inputs and outputs have different scales that affect the
 259 sensitivity and convergence of the developed surrogate models, they are both normalized from
 260 0 to 1, using the min-max scaling equation (3):

$$y'_i = \frac{y_i - \min(y_i)}{\max(y_i) - \min(y_i)} \quad (3)$$

261 Where y'_i is the normalized value of y_i variable.

262 Table 2. Upper and lower limits of optimization variables.

Optimization variables (x)	Lower bound (x_{min})	Upper bound (x_{max})
x_1 : Acid loading (mg/g dry biomass)	1	2
x_2 : Pretreatment temperature (°C)	155	185
x_3 : Pretreatment residence time (min)	1	20
x_4 : Feed (dry t/d)	80	2000
x_5 : Saccharification residence time (min)	10	120
x_6 : Fermentation residence time (min)	10	50

263

264 2.5.2 ANN development

265 First, the architecture of the ANN is studied and optimized for each objective. In this
 266 study, only shallow and two-hidden layers ANNs are considered due to their simplicity. The
 267 number and size of layers are optimized, taking a maximum number of neurons per layer as
 268 double the amount of inputs based on rules-of-thumb [36], that being 12. The mean squared
 269 error (MSE) is used as the performance criterion to select the optimal ANN architecture:

$$MSE = \frac{1}{n} \sum_{i=1}^n (J_i - \tilde{J}_i)^2 \quad (4)$$

270 Where n is the number of samples, J_i is the real value and \tilde{J}_i is the predicted value.

271 The ANN models are developed in MATLAB R2022b, using the *fitnet* function of the
272 Deep Learning Toolbox. The training data are partitioned into training, validation and testing
273 sets at a 70%, 20% and 10% ratio respectively. The Levenberg-Marquardt training method is
274 chosen, while the rest of the training parameters are kept the same as the default options.

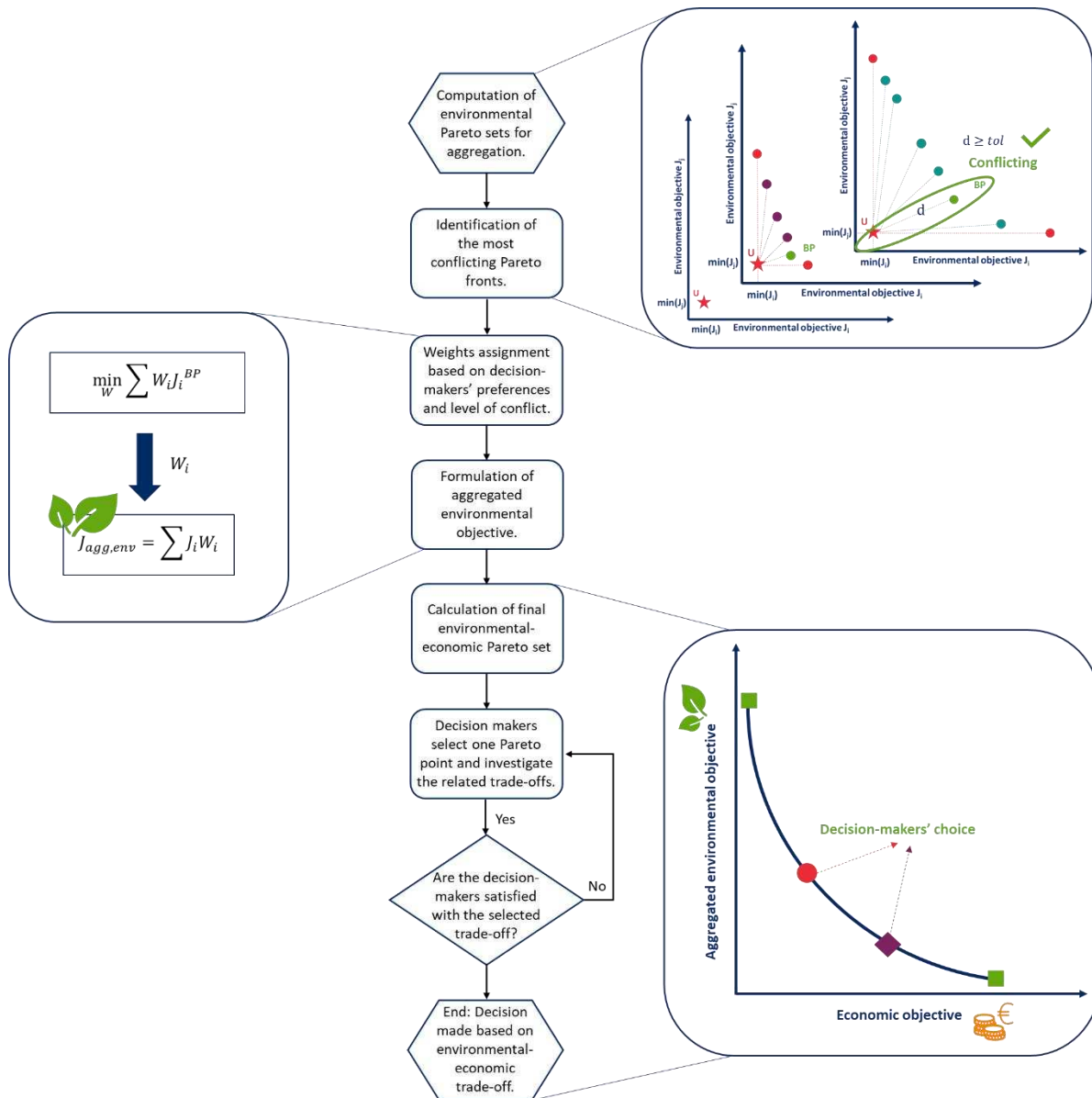
275 2.6 Pareto aggregation algorithm

276 The proposed Pareto aggregation algorithm is presented in Figure 2. First, multiple bi-
277 objective Pareto fronts are computed for each unique combination of two environmental
278 objectives. The number of Pareto fronts N is calculated by equation (5):

$$N(n_{J_{env}}, k) = \frac{n_{J_{env}}!}{k! (n_{J_{env}} - k)!} \quad (5)$$

279 Where $n_{J_{env}}$ is the number of environmental objectives and k is the number of objectives for
280 each combination. In this work, the environmental objectives are $n_{J_{env}} = 18$: $J_{env} = \{J_i \mid i =$
281 $2, \dots, 19\}$. For 18 environmental indicators taken two at a time, 153 Pareto fronts are required.

282 Then, the most conflicting objectives are identified based on specific criteria, and
283 weights are generated as described in the following subsections. This way the optimization is
284 focused on finding solutions that balance the conflicting objectives first, leading to more robust
285 results. Finally, the aggregated environmental objective is formed and traded-off against the
286 economic objective J_1 .



287

288 Figure 2. Schematic representation of the Pareto aggregation algorithm (BP: Best point, U:
 289 Utopia point, d: Euclidean distance between BP and U, *tol*: tolerance value, W: Weights used
 290 for aggregation).

291 2.6.1 Identification of conflicting objectives

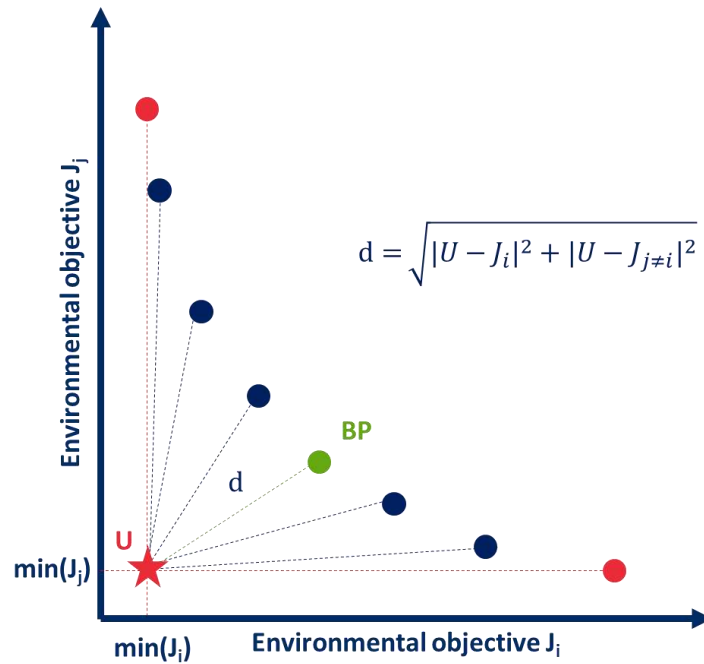
292 The most conflicting objectives $J_i \in J_{env}$ are identified using the following criteria:

- 293 1. The Pareto front should consist of more than one point.

294 2. The minimum Euclidian distance of the Pareto points from the Utopia point should be greater
 295 than a tolerance value:

$$\min \left\{ \sqrt{|U - J_i|^2 + |U - J_{j \neq i}|^2} \right\} \geq tol, \quad J_i, J_{j \neq i} \in J_{env} \quad (6)$$

296 Where $U = (\min(J_i), \min(J_{j \neq i}))$ is the Utopia point and tol is the tolerance value. The Utopia
 297 point consists of the individual minima of each objective function. The tol parameter can be
 298 specified by the decision-maker, reflecting what is defined as conflicting. Indeed, its value can
 299 be varied to make the criterion more or less strict. In this study, a tolerance of 10^{-3} is deemed
 300 as suitable, as the objective values are normalized from 0 to 1. The point of each Pareto front
 301 that satisfies the left part of equation (6) is hereby mentioned as “Best point” (BP). A simplified
 302 example is given in Figure 3.



303
 304 Figure 3. Environmental Pareto front for aggregation between objectives J_i and J_j . U is the
 305 Utopia point, BP the Best point and d the distance of each Pareto point from U.

306 By satisfying both of these criteria, the most conflicting objectives (J_{conf}) are identified,
 307 with $J_{conf} \subseteq J_{env}$. The number of conflicting objectives is n_{JC} corresponding to PF_{JC} Pareto
 308 fronts.

309 2.6.2 Weights generation

310 The final aggregation of the most conflicting environmental objectives can be done
 311 through a weighted sum method:

$$J_{agg,env} = \sum_{i \in [2,19] | J_i \in J_{conf}} J_i W_i \quad (7)$$

312 Where W_i is the weight of the conflicting objective $J_i \in J_{conf}$, with $\sum_{i \in [2,19] | J_i \in J_{conf}} W_i = 1$.

313 For the generation of the weights, a novel approach is suggested that accounts for
 314 decision-makers' preferences (if available) and/or the level of conflict between the objectives.
 315 Higher weights can be assigned to objectives that are more important to decision-makers and
 316 are highly conflicting:

$$\begin{aligned} \min_W \quad & \sum_{i \in [2,19] | J_i \in J_{conf}} W_i J_i^{BP} \quad (8) \\ \text{s.t.} \quad & \sum_{i \in [2,19] | J_i \in J_{conf}} W_i = 1 \\ & A \cdot W \leq b \\ & c(W) \leq 0 \\ & 0.01 \leq W \leq 1 \end{aligned}$$

317 Where W is a vector containing the weights, J_i^{BP} are the objective values on the Best Point
 318 (BP) of $J_i \in J_{conf}$, A is a matrix, b a vector and $c(W)$ a nonlinear inequality function that returns

319 a vector. The values of A and b can be chosen in order to reflect the decision-makers'
320 preferences and/or the level of conflict between the objectives. The nonlinear inequalities are
321 taken as $c(W) = (J_i^{BP} - WJ_i^{BP})^2 - 10^{-8} \leq 0$, ensuring that the weight generation is not
322 significantly influenced by the absolute values of the objectives (e.g. extremely high weights
323 assigned to low objective values). For the same reason, the lower bound of the weights is taken
324 as 0.01 in order to guarantee that high objective values J_i^{BP} are not given extremely low
325 weights, close to 0 (e.g. 10^{-6} - 10^{-4}). The *fmincon* MATLAB function is applied, using the default
326 options of the Interior Point Method.

327 **3. RESULTS AND DISCUSSION**

328 3.1 Surrogate modelling results

329 The 6D design space was sampled 5000 times using the Best Candidate algorithm [34],
330 requiring 470 seconds of running time. Detailed results on its performance are available in the
331 Supplementary Material. ANNs were then used to create 20 surrogate models in total between
332 the optimization variables and the optimization objectives; one for each out of the 19 ReCiPe
333 environmental indicators and one for the EcoIndicator99. The optimal architecture, identified
334 through the calculation of MSE, was found for each surrogate model, as shown in Table 3.
335 Mean squared errors in the magnitude of 10^{-5} - 10^{-6} were achieved for all models for a two-
336 layered ANN. The coefficients of determination (R^2) for the training, validation, testing total
337 data are also shown in Table 3. These are higher than 99% for all models and data, indicating
338 good predictions and that surrogate models are able to capture the relationships between the
339 objective functions and optimization variables.

340 Table 3. Performance and architecture of the optimal ANN for each surrogate model/objective function. R^2 train, R^2 val, R^2 test and R^2 total are
 341 the coefficients of determination for the training, validation, testing and total data respectively.

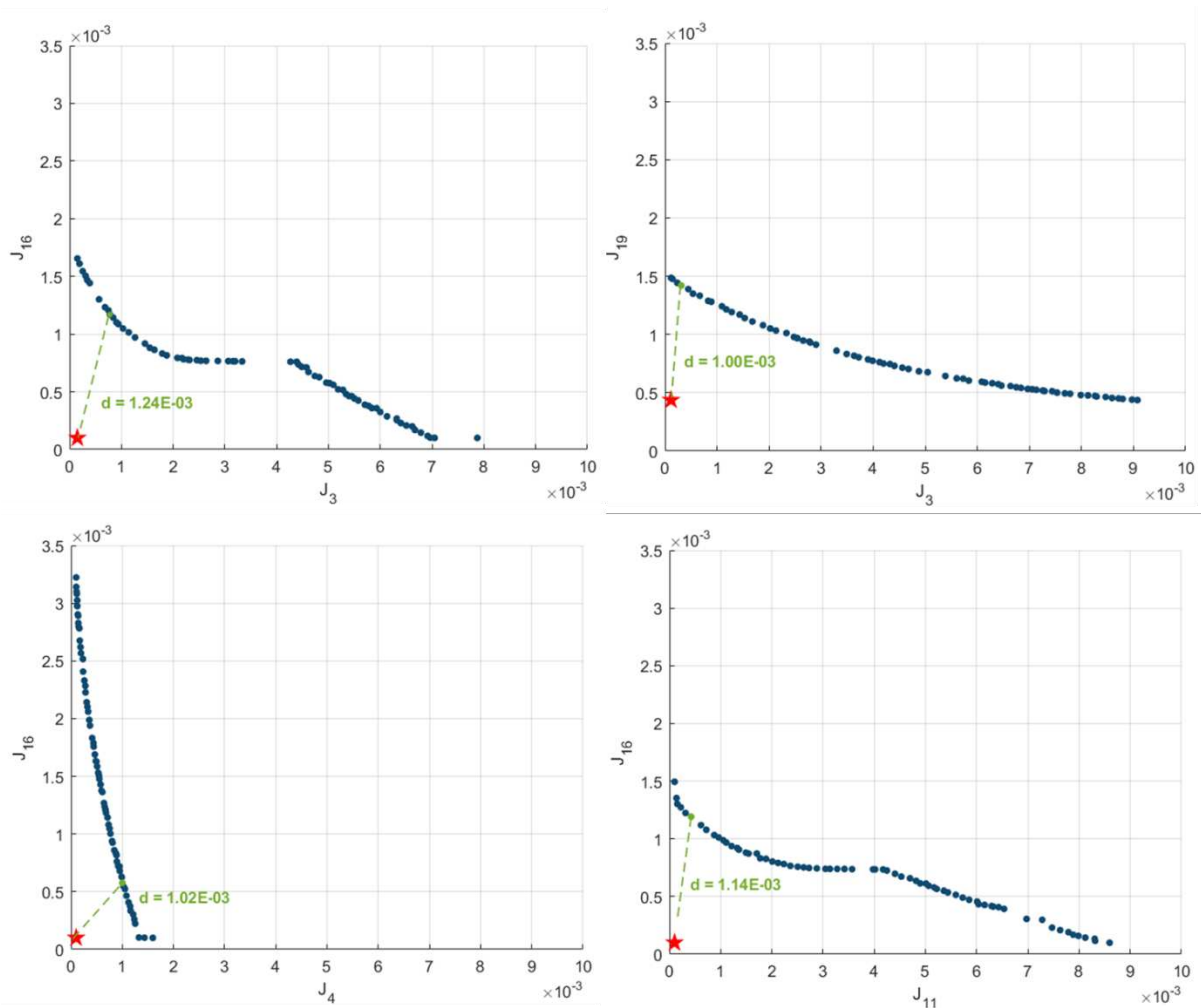
Surrogate model/Objective function	MSE	R^2 train	R^2 val	R^2 test	R^2 total	No of neurons in 1 st layer	No of neurons in 2 nd layer
J_1	8.36e-06	0.9992	0.9995	0.9997	0.9993	10	8
J_2	1.70e-05	0.9999	0.9976	0.9997	0.9995	11	9
J_3	9.65e-06	0.9993	0.9998	0.9997	0.9995	12	10
J_4	2.58e-06	0.9998	0.9986	0.9997	0.9995	12	6
J_5	1.40e-05	0.9999	0.9998	0.9956	0.9995	11	7
J_6	1.47e-05	0.9992	0.9997	0.9996	0.9995	10	6
J_7	1.38e-05	0.9992	0.9998	0.9998	0.9995	11	9
J_8	1.64e-05	0.9992	0.9994	0.9997	0.9995	11	7
J_9	1.29e-05	0.9993	0.9997	0.9998	0.9995	12	7
J_{10}	1.23e-05	0.9993	0.9998	0.9997	0.9995	11	6
J_{11}	1.29e-05	0.9993	0.9998	0.9998	0.9995	12	8
J_{12}	7.82e-06	0.9994	0.9998	0.9998	0.9995	12	10
J_{13}	1.07e-05	0.9998	0.9997	0.9955	0.9995	11	8
J_{14}	9.56e-06	0.9993	0.9998	0.9997	0.9995	12	5
J_{15}	9.99e-06	0.9993	0.9997	0.9997	0.9995	11	9
J_{16}	1.12e-05	0.9999	0.9979	0.9999	0.9995	12	7
J_{17}	7.74e-06	0.9999	0.9981	0.9998	0.9995	12	9
J_{18}	1.45e-05	0.9999	0.9998	0.9962	0.9995	12	10
J_{19}	1.64e-05	0.9999	0.9974	0.9984	0.9995	12	9
J_{20}	1.25e-05	0.9999	0.9977	0.9998	0.9994	12	9

342

343 3.2 Pareto aggregation results

344 In total, 153 Pareto fronts were calculated for 18 environmental indicators. Out of these,
345 four ($PF_{JC} = 4$) were found to be conflicting based on the criteria specified in the Pareto
346 aggregation algorithm. In Figure 4, the minimum distance calculated between the Pareto points
347 and the Utopia point (U) is depicted, that being equal or higher to 10^{-3} . Therefore, five
348 environmental indicators are identified as the most conflicting, those being the stratospheric
349 ozone depletion (J_3), ionizing radiation (J_4), terrestrial ecotoxicity (J_{11}), land use (J_{16}) and water
350 consumption (J_{19}).

351 It is evident from Figure 4 that land use (J_{16}) is highly conflicting with stratospheric
352 ozone depletion (J_3) and terrestrial ecotoxicity (J_{11}), while water consumption (J_{19}) has the least
353 conflicting relation with stratospheric ozone depletion (J_3). Based on these observations and
354 given the lack of decision-makers' preference in the current case study, the linear inequalities
355 of equation (8) are chosen, assigning higher weights to the most conflicting objectives, those
356 being J_{16} , followed by J_3 and J_{11} .



357

358 Figure 4. Conflicting objectives identified through the Pareto aggregation algorithm: (A)
 359 Stratospheric ozone depletion (J_3) vs Land use (J_{16}), (B) Stratospheric ozone depletion (J_3) vs
 360 Water consumption (J_{19}), (C) Ionizing radiation (J_4) vs Land use (J_{16}) and (D) Terrestrial
 361 ecotoxicity (J_{11}) vs Land use (J_{16}). The distance (d) between the Utopia Point (★) and the Best
 362 Point (●) is also shown. Both objective values are normalized within $[0,1]$.

363 The identified conflicting behaviour can be explained by the fact that corn stover has
 364 the highest emission factor for land use, which on the other hand has an insignificant emission
 365 factor for stratospheric ozone depletion, ionizing radiation and terrestrial ecotoxicity, which are
 366 mostly affected by the diammonium phosphate and electricity supply. Indeed, ozone depletion
 367 and ionizing radiation get both minimized at a very low fermentation residence time, almost

368 three times less than the one for land use, due to the high impact of diammonium phosphate
 369 consumption. Similarly, water consumption indicator is mostly affected by the wastewater
 370 output, resulting in around 30% less acid loading required for the minimization of this indicator
 371 compared to the rest.

372 The final weights for each objective are presented in Table 4. Land use has the highest
 373 contribution to the final environmental objective, followed by stratospheric ozone depletion,
 374 terrestrial ecotoxicity, ionizing radiation and water consumption. The performance and
 375 reliability of the proposed weight generation algorithm has been verified through a robustness
 376 check (details in Supporting Material).

377 Table 4. Weights assigned to the most conflicting environmental objectives

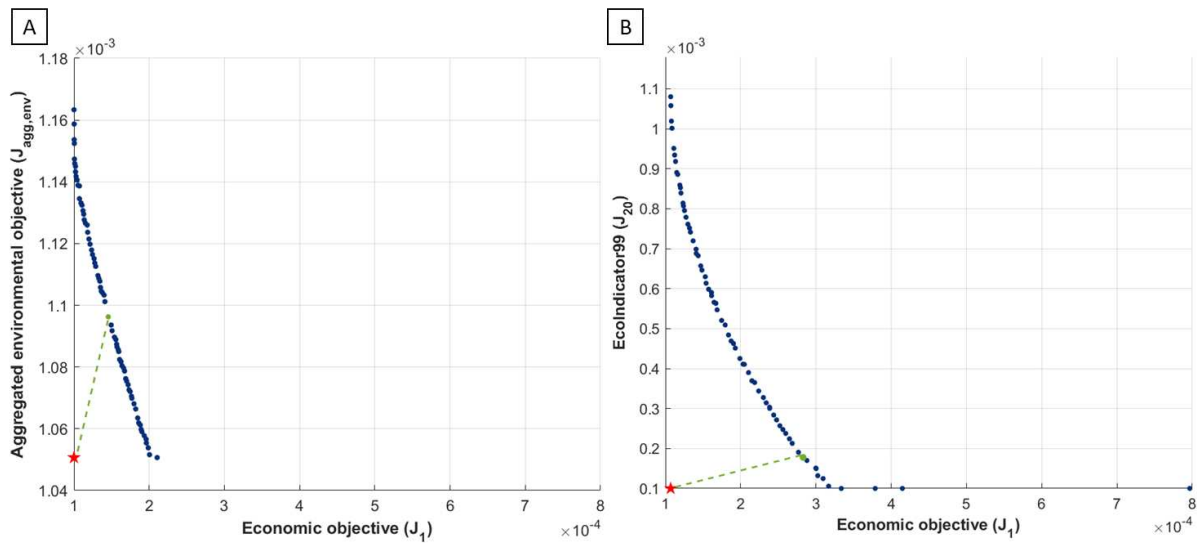
Environmental objective	Weight
Stratospheric ozone depletion (J_3)	0.3159
Ionizing radiation (J_4)	0.0107
Terrestrial ecotoxicity (J_{11})	0.2546
Land use (J_{16})	0.3188
Water consumption (J_{19})	0.1000
Sum	1.0000

378

379 3.3 Environmental-economic multi-objective optimization results

380 The aggregated environmental objective $J_{agg,env}$ was then traded-off against the economic
 381 objective J_1 . The final Pareto front is presented in Figure 5(A), obtained for 1200 maximum
 382 number of iterations and population size taken as 200. A conflicting relationship between the
 383 chosen economic objective and the aggregated environmental objective is identified. Detailed
 384 results of the optimization variables can be found in the Supporting Material.

385



386

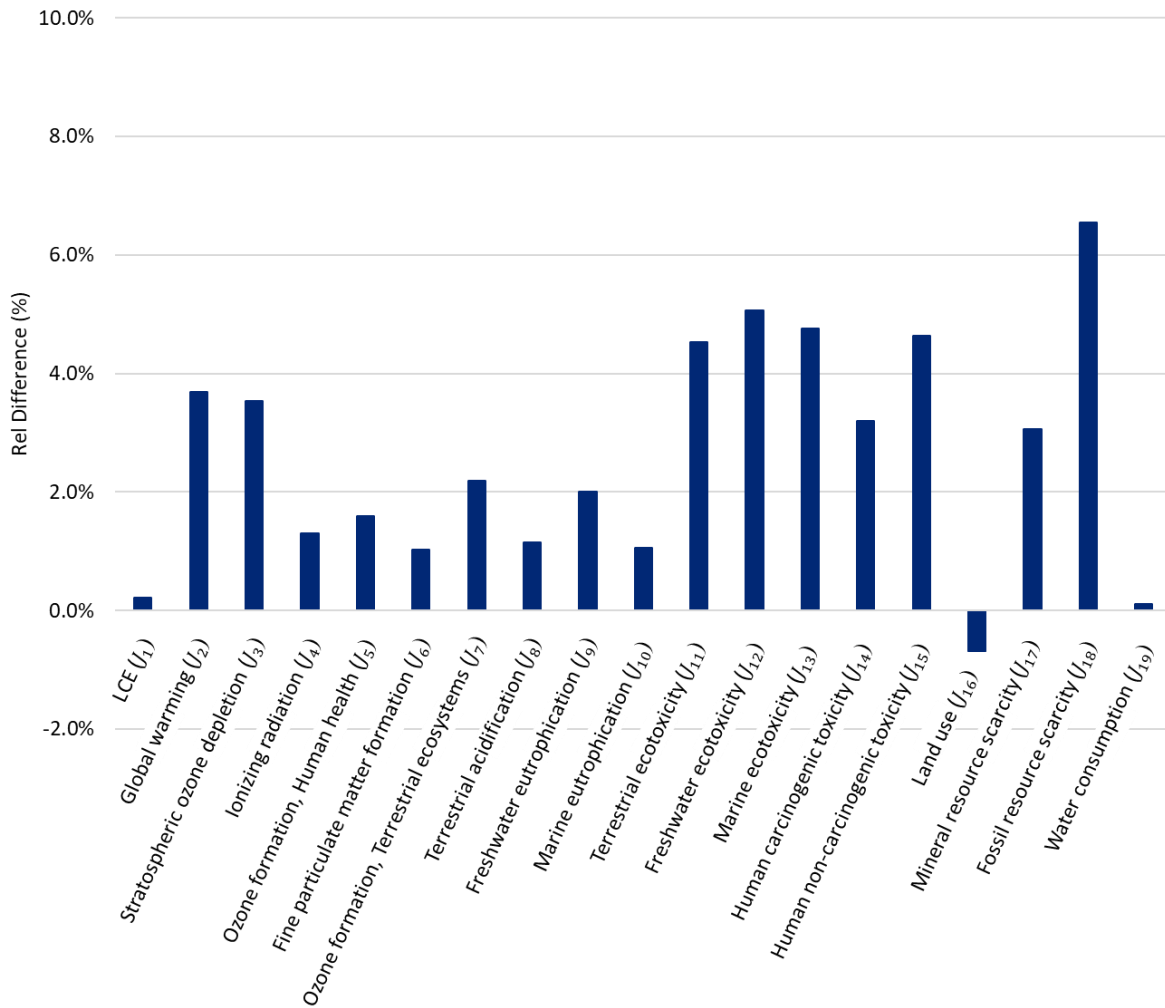
387 Figure 5. Final environmental-economic Pareto front of the (A) Aggregated environmental
388 objective ($J_{agg,env}$) and (B) EcoIndicator99 (J_{20}). The Utopia Point (★) and the Best Point (●)
389 are also depicted. All objectives are normalized within [0,1].

390 As far as the optimization variables are concerned, a high biomass feed is required for
391 all of the Pareto optimal solutions, around 1800 dry t/d biomass on average, as the scale of the
392 biorefinery has a significant effect in the economic performance (economies of scale) [37]. A
393 high acid loading (~ 2.0 mg/g dry biomass) accompanied by low temperature ($\sim 159^\circ\text{C}$) and high
394 residence time (~ 20 min) is required for the acid pretreatment process. The low pretreatment
395 temperature influences both the economic and environmental performance, as less inhibitors
396 are produced while limiting the energy consumption. A high saccharification time (~ 120 min)
397 is also required in order to achieve a high sugar conversion, while the fermentation time is
398 significantly lower, varying from 35 to 39 min. This can be explained by the fact that after 30
399 min most of the sugars are already converted to ethanol [29].

400 In order to validate the aggregation approach proposed in this study, a comparison with
401 a commonly used environmental single-score indicator, EcoIndicator99, has been conducted.

402 The Pareto front obtained for trading the economic objective against the EcoIndicator99 is
403 presented in Figure 5 (B).

404 The optimization objective values (non-normalized) on the Best Point of each Pareto
405 front were calculated, allowing for a more comprehensible comparison. The relative difference
406 between the two Pareto fronts for all optimization objectives is presented in Figure 6. It is now
407 evident that almost all of the environmental objectives are lower by applying the Pareto
408 aggregation algorithm compared to the EcoIndicator99, except for the Land Use (J_{16}) which is
409 however insignificantly higher, less than 1%. Notably, Fossil resource scarcity (J_{18}) can be
410 reduced by 6.5%, Freshwater ecotoxicity (J_{12}) by 5.1% and Marine ecotoxicity (J_{13}) by 4.8%
411 by applying the Pareto aggregation algorithm. For both MOOs, the same value on the economic
412 objective (LCE) was obtained, that being 1.25 EUR/L.



414

415 Figure 6. Relative difference between optimization objectives on the Best Point (BP) of the

416 Economic-Aggregated environmental objective ($J_i^{BP,agg}$) and the Economic-EcoIndicator99

417 ($J_i^{BP,EI99}$) Pareto fronts. Relative difference calculated as: $\frac{J_i^{BP,EI99} - J_i^{BP,agg}}{J_i^{BP,agg}}$.

418 These final environmental objectives on the Best point can be attained by decreasing the

419 acid pretreatment temperature by 7°C, while increasing the feed by 47 dry t/d and the

420 fermentation time by 3 min, compared to the EcoIndicator99 results. The rest of the

421 optimization variables are almost the same. Detailed results on the optimization variables and
422 objectives for both Pareto fronts can be found in the Supplementary Material.

423 3.4 Discussion

424 The Pareto aggregation method suggested in this study is especially designed to tackle
425 in a systematic way MOO problems which are normally solved via aggregation. This is done
426 by identifying truly conflicting optimization objectives and performing an aggregation of those
427 while taking into consideration their level of conflict and/or decision-makers' preferences, if
428 available.

429 This method allows the practitioner to account for multiple indicators that are available
430 to describe a single performance (e.g., economic, environmental, social). Nevertheless, the
431 identification of conflicting indicators before the final multi-objective optimization can
432 significantly reduce the dimensionality of the optimization problem. That was indeed illustrated
433 by the applied case study on a lignocellulosic biorefinery, as only five out of the eighteen in
434 total environmental indicators were found to be conflicting and an aggregation between those
435 was required.

436 Moreover, the criteria used for the identification of the most conflicting objectives are
437 subjected to the practitioners' priorities, and can be adjusted to make the algorithm more or less
438 rigorous. Thus, the tolerance value required by the algorithm (equation (6)) should be carefully
439 chosen based on the case study and desired outcome. Similarly, the weight generation approach
440 is highly dependent on particular parameters specified by the practitioner. It is thus evident that
441 another advantage of the proposed method is that it can easily be adjusted to take into
442 consideration and reflect both practitioners' and decision-makers' preferences.

443 3.4.1 Method applicability

444 The developed method was illustrated on an environmental-economic multi-objective
445 optimization problem, as the aggregation issue involved in environmental assessments has been
446 widely discussed in literature [38]. However, its usage can be further expanded and applied to
447 different types of multi-objective optimization problems that require an aggregation of multiple
448 indicators. Based on the obtained results, decisions can be made on the operating conditions of
449 a lignocellulosic bioethanol plant, to minimize the final production cost, while, at the same
450 time, supporting a more environmentally sustainable performance. For the chosen case study,
451 a large plant capacity in addition to low pretreatment time and high saccharification time can
452 achieve a large ethanol production, and thus a low production cost (economies of scale),
453 accompanied by a low environmental impact (less inhibitors production). It can thus serve as a
454 quantitative tool in decision-making processes, exploring the relationship between different
455 objectives and guiding decision-makers to select optimal operating parameters based on their
456 own priorities. Such decision-making processes are critical for energy technologies, covering
457 both energy generation and management, as technical, economic, environmental and social
458 objectives need to be satisfied [4].

459 The suggested Pareto aggregation method can easily be applied to different case studies.
460 The only requirement is the development of a dynamic model that describes the relationship
461 between the optimization variables and the optimization objectives. For process engineering,
462 this relationship is usually expressed through detailed mass & energy balance calculations. For
463 complex processes, process simulation software, such as ASPEN Plus used in this study, are
464 commonly used to facilitate these calculations. Then, the Pareto aggregation method, i.e. the
465 third step (C) in Figure 1, can be easily applied. In case of computationally expensive models,
466 parallel computing and/or surrogate models (e.g., ANNs used in this study) could help reduce
467 running times.

468 3.4.2 Limitations & Future work

469 It is worth mentioning that any uncertainties related to the models applied were not taken
470 into consideration and left out of the scope of this study. However, these uncertainties do not
471 have a direct effect on the suggested method itself, but rather on the final case study-specific
472 results. In future work, the proposed Pareto aggregation algorithm could also be embedded in
473 an interactive multi-objective optimization framework, and the inherent uncertainties of the
474 models should also be taken into account, as these may affect the process [39]. The inclusion
475 of uncertainties could be done by using uncertainty propagation techniques such as
476 linearization, sigma points (unscented transformation) and polynomial chaos expansion to
477 propagate the uncertainty on the model parameters towards the objective functions and
478 constraint functions, as explained by e.g., Nimmegeers et al. [40], and Mores et al. [41].
479 Nevertheless, the application of the suggested method to different case studies, as explained in
480 section 3.4.1, could help to further improve and operationalize it.

481 4. CONCLUSIONS

482 A novel method, named Pareto aggregation, is suggested for generating an
483 environmental objective function, by identifying the most conflicting environmental indicators.
484 This method was applied to a bioethanol production plant in an economic-environmental multi-
485 objective optimization. Surrogate models were developed based on simulation and kinetic
486 models. Five environmental indicators, namely stratospheric ozone depletion, ionizing
487 radiation, terrestrial ecotoxicity, land use and water consumption, were identified as conflicting.
488 Based on the level of conflict, an aggregated environmental objective was developed and
489 traded-off against an economic objective, that being the levelized cost of ethanol. The final
490 Pareto optimal solutions obtained indicate the best performance possibilities for the investigated
491 biorefinery. The method was compared against the single-score EcoIndicator99, demonstrating

492 a better performance as a decrease ranging from 1.0 to 6.5% was observed for almost all
493 indicators calculated through the Pareto aggregation method. This approach can significantly
494 reduce the multi-dimensionality of optimization problems and can be easily applied to other
495 energy systems, serving as a useful tool in decision-making processes when multiple objectives
496 need to be satisfied..

497 **ACKNOWLEDGMENTS**

498 This study was carried out within the framework of the ADV_BIO project financed by the FOD
499 Economie - Energietransitiefonds/ SPF Économie - Fonds de Transition Energétique, call 2019
500 - 2020 subsidies. Philippe Nimmegeers holds a FWO senior postdoctoral fellowship (grant
501 number: 1215523N) granted by FWO Vlaanderen/Research Foundation Flanders.

502 **APPENDIX A. SUPPLEMENTARY DATA**

503 Supplementary data to this article can be found online: <Supplementary Material>

504 **REFERENCES**

- 505 [1] Rangaiah G, Sharma S, Sreepathi BK. Multi-objective optimization for the design
506 and operation of energy efficient chemical processes and power generation. *Curr*
507 *Opin Chem Eng* 2015;10:49–62. <https://doi.org/10.1016/j.coche.2015.08.006>.
- 508 [2] Schweidtmann AM, Clayton AD, Holmes N, Bradford E, Bourne RA, Lapkin AA.
509 Machine learning meets continuous flow chemistry: Automated optimization
510 towards the Pareto front of multiple objectives. *Chem Eng J* 2018;352:277–82.
511 <https://doi.org/10.1016/j.cej.2018.07.031>.
- 512 [3] Cheraghi R, Hossein Jahangir M. Multi-objective optimization of a hybrid
513 renewable energy system supplying a residential building using NSGA-II and

- 514 MOPSO algorithms. *Energy Convers Manag* 2023;294:117515.
515 <https://doi.org/10.1016/j.enconman.2023.117515>.
- 516 [4] Al Moussawi H, Fardoun F, Louahlia-Gualous H. Review of tri-generation
517 technologies: Design evaluation, optimization, decision-making, and selection
518 approach. *Energy Convers Manag* 2016;120:157–96.
519 <https://doi.org/10.1016/j.enconman.2016.04.085>.
- 520 [5] Čuček L, Klemeš JJ, Kravanja Z. A Review of Footprint analysis tools for
521 monitoring impacts on sustainability. *J Clean Prod* 2012;34:9–20.
522 <https://doi.org/https://doi.org/10.1016/j.jclepro.2012.02.036>.
- 523 [6] Cheraghi R, Hossein Jahangir M. Multi-objective optimization of a hybrid
524 renewable energy system supplying a residential building using NSGA-II and
525 MOPSO algorithms. *Energy Convers Manag* 2023;294:117515.
526 <https://doi.org/10.1016/j.enconman.2023.117515>.
- 527 [7] Das BK, Hassan R, Tushar MSHK, Zaman F, Hasan M, Das P. Techno-economic
528 and environmental assessment of a hybrid renewable energy system using multi-
529 objective genetic algorithm: A case study for remote Island in Bangladesh. *Energy
530 Convers Manag* 2021;230:113823.
531 <https://doi.org/10.1016/j.enconman.2020.113823>.
- 532 [8] Afrinaldi F, Zhang H-C. A fuzzy logic based aggregation method for life cycle
533 impact assessment. *J Clean Prod* 2014;67:159–72.
534 <https://doi.org/10.1016/j.jclepro.2013.12.010>.
- 535 [9] Goedkoop M, Spriensma R. *The Eco-Indicator 99: A Damage Oriented Method
536 for Life Cycle Impact Assessment* 2001.

- 537 [10] Le Roux D, Lalau Y, Rebouillat B, Neveu P, Olivès R. Thermocline thermal
538 energy storage optimisation combining exergy and life cycle assessment. *Energy*
539 *Convers Manag* 2021;248:114787.
540 <https://doi.org/10.1016/j.enconman.2021.114787>.
- 541 [11] Hafizan C, Noor ZZ, Abba AH, Hussein N. An alternative aggregation method
542 for a life cycle impact assessment using an analytical hierarchy process. *J Clean*
543 *Prod* 2016;112:3244–55. <https://doi.org/10.1016/j.jclepro.2015.09.140>.
- 544 [12] Agarski B, Budak I, Vukelic D, Hodolic J. Fuzzy multi-criteria-based impact
545 category weighting in life cycle assessment. *J Clean Prod* 2016;112:3256–66.
546 <https://doi.org/10.1016/j.jclepro.2015.09.077>.
- 547 [13] Sohn J, Bisquert P, Buche P, Hecham A, Kalbar PP, Goldstein B, et al.
548 Argumentation Corrected Context Weighting-Life Cycle Assessment: A Practical
549 Method of Including Stakeholder Perspectives in Multi-Criteria Decision Support
550 for LCA. *Sustainability* 2020;12:2170. <https://doi.org/10.3390/su12062170>.
- 551 [14] Azapagic A, Clift R. The application of life cycle assessment to process
552 optimisation. vol. 23. 1999.
- 553 [15] Ayres RU. Commentary on the utility of the ecological footprint concept. vol. 32.
554 2000.
- 555 [16] Zacharopoulos L, Thonemann N, Dumeier M, Geldermann J. Environmental
556 optimization of the charge of battery electric vehicles. *Appl Energy*
557 2023;329:120259. <https://doi.org/10.1016/j.apenergy.2022.120259>.

- 558 [17] Arfan M, Eriksson O, Wang Z, Soam S. Life cycle assessment and life cycle
559 costing of hydrogen production from biowaste and biomass in Sweden. *Energy*
560 *Convers Manag* 2023;291:117262.
561 <https://doi.org/10.1016/j.enconman.2023.117262>.
- 562 [18] Lee D, Nam H, Won Seo M, Hoon Lee S, Tokmurzin D, Wang S, et al. Recent
563 progress in the catalytic thermochemical conversion process of biomass for
564 biofuels. *Chem Eng J* 2022;447:137501.
565 <https://doi.org/10.1016/j.cej.2022.137501>.
- 566 [19] Yong KJ, Wu TY. Second-generation bioenergy from oilseed crop residues:
567 Recent technologies, techno-economic assessments and policies. *Energy Convers*
568 *Manag* 2022;267:115869. <https://doi.org/10.1016/j.enconman.2022.115869>.
- 569 [20] Moodley P, Gueguim Kana EB. Development of a steam or microwave-assisted
570 sequential salt-alkali pretreatment for lignocellulosic waste: Effect on
571 delignification and enzymatic hydrolysis. *Energy Convers Manag* 2017;148:801–
572 8. <https://doi.org/10.1016/j.enconman.2017.06.056>.
- 573 [21] Rangaiah G, Sharma S, Sreepathi BK. Multi-objective optimization for the design
574 and operation of energy efficient chemical processes and power generation. *Curr*
575 *Opin Chem Eng* 2015;10:49–62. <https://doi.org/10.1016/j.coche.2015.08.006>.
- 576 [22] Jeon PR, Moon J-H, Ogunsola NO, Lee SH, Ling JLJ, You S, et al. Recent
577 advances and future prospects of thermochemical biofuel conversion processes
578 with machine learning. *Chem Eng J* 2023;471:144503.
579 <https://doi.org/10.1016/j.cej.2023.144503>.
- 580 [23] Aspen Technology I. ASPEN Plus V12.1 2021.

- 581 [24] Humbird D, Davis R, Tao L, Kinchin C, Hsu D, Aden A, et al. Process Design
582 and Economics for Biochemical Conversion of Lignocellulosic Biomass to
583 Ethanol: Dilute-Acid Pretreatment and Enzymatic Hydrolysis of Corn Stover.
584 Golden, CO (United States): 2011. <https://doi.org/10.2172/1013269>.
- 585 [25] Shi S, Guan W, Kang L, Lee YY. Reaction kinetic model of dilute acid-catalyzed
586 hemicellulose hydrolysis of corn stover under high-solid conditions. *Ind Eng*
587 *Chem Res* 2017;56:10990–7. <https://doi.org/10.1021/acs.iecr.7b01768>.
- 588 [26] Lavarack BP, Griffin GJ, Rodman D. The acid hydrolysis of sugarcane bagasse
589 hemicellulose to produce xylose, arabinose, glucose and other products. *Biom*
590 *Bioen* 2002;23:367–80. [https://doi.org/10.1016/S0961-9534\(02\)00066-1](https://doi.org/10.1016/S0961-9534(02)00066-1).
- 591 [27] Humbird D, Aden A. Biochemical Production of Ethanol from Corn Stover: 2008
592 State of Technology Model. Technical Report NREL/TP-510-46214: 2009.
- 593 [28] Kadam KL, Rydholm EC, McMillan JD. Development and Validation of a Kinetic
594 Model for Enzymatic Saccharification of Lignocellulosic Biomass. *Biotechnol*
595 *Prog* 2004;20:698–705. <https://doi.org/10.1021/bp034316x>.
- 596 [29] Leksawasdi N, Joachimsthal EL, Rogers PL. Mathematical modelling of ethanol
597 production from glucose/xylose mixtures by recombinant *Zymomonas mobilis*.
598 *Biotechnol Lett* 2001;23:1087–93. <https://doi.org/10.1023/A:1010599530577>.
- 599 [30] Moomaw W, Burgherr P, Heath G, Lenzen M, Nyboer J, Verbruggen A. Annex
600 II: Methodology. . In IPCC Special Report on Renewable Energy Sources and
601 Climate Change Mitigation [O. Edenhofer, R. Pichs-Madruga, Y. Sokona, K.
602 Seyboth, P. Matschoss, S. Kadner, T. Zwickel, P. Eickemeier, G. Hansen, S.

- 603 Schlömer, C. von Stechow (eds)]. Cambridge, United Kingdom and New York,
604 NY, USA: 2011.
- 605 [31] Wernet G, Bauer C, Steubing B, Reinhard J, Moreno-Ruiz E, Weidema B. The
606 ecoinvent database version 3 (part I): overview and methodology. *Int J Life Cycle*
607 *Assess* 2016;21:1218–30. <https://doi.org/10.1007/s11367-016-1087-8>.
- 608 [32] Huijbregts MAJ, Steinmann ZJN, Elshout PMF, Stam G, Verones F, Vieira
609 MDM, et al. ReCiPe2016. A harmonized life cycle impact assessment method at
610 midpoint and endpoint level. Report I: Characterization. RIVM Report 2016-
611 0104. Bilthoven: 2017.
- 612 [33] Fozer D, Nimmegeers P, Toth AJ, Varbanov PS, Klemeš JJ, Mizsey P, et al.
613 Hybrid Prediction-Driven High-Throughput Sustainability Screening for
614 Advancing Waste-to-Dimethyl Ether Valorization. *Environ Sci Technol*
615 2023;57:13449–62. <https://doi.org/10.1021/acs.est.3c01892>.
- 616 [34] Mitchell DP. Spectrally optimal sampling for distribution ray tracing. *Proceedings*
617 *of the 18th annual conference on Computer graphics and interactive techniques -*
618 *SIGGRAPH '91*, New York, New York, USA: ACM Press; 1991, p. 157–64.
619 <https://doi.org/10.1145/122718.122736>.
- 620 [35] Kamath C. Intelligent sampling for surrogate modeling, hyperparameter
621 optimization, and data analysis. *Machine Learning with Applications*
622 2022;9:100373. <https://doi.org/10.1016/j.mlwa.2022.100373>.
- 623 [36] Berry MJA, Linoff GS. *Data Mining Techniques For Marketing, Sales, and*
624 *Customer Relationship Management*. 2nd ed. Wiley Publishing Inc.; 2004.

- 625 [37] Vasilakou K, Nimmegeers P, Thomassen G, Billen P, Van Passel S. Assessing the
626 future of second-generation bioethanol by 2030 – A techno-economic assessment
627 integrating technology learning curves. *Appl Energy* 2023;344:121263.
628 <https://doi.org/10.1016/j.apenergy.2023.121263>.
- 629 [38] Kalbar PP, Birkved M, Nygaard SE, Hauschild M. Weighting and Aggregation in
630 Life Cycle Assessment: Do Present Aggregated Single Scores Provide Correct
631 Decision Support? *J Ind Ecol* 2017;21:1591–600.
632 <https://doi.org/10.1111/jiec.12520>.
- 633 [39] Nimmegeers P, Vallerio M, Telen D, Van Impe J, Logist F. Interactive Multi-
634 objective Dynamic Optimization of Bioreactors under Parametric Uncertainty.
635 *Chemie Ingenieur Technik* 2019;91:349–62.
636 <https://doi.org/10.1002/cite.201800082>.
- 637 [40] Nimmegeers P, Telen D, Logist F, Impe J Van. Dynamic optimization of
638 biological networks under parametric uncertainty. *BMC Syst Biol* 2016;10:86.
639 <https://doi.org/10.1186/s12918-016-0328-6>.
- 640 [41] Mores W, Nimmegeers P, Hashem I, Bhonsale SS, Van Impe JFM. Multi-
641 objective optimization under parametric uncertainty: A Pareto ellipsoids-based
642 algorithm. *Comput Chem Eng* 2023;169:108099.
643 <https://doi.org/10.1016/j.compchemeng.2022.108099>.

644